

Empirical indoor-to-outdoor propagation model for residential areas at (0.9 - 3.5) GHz

Alvaro Valcarce, *Student Member, IEEE* and Jie Zhang, *Member, IEEE*

Abstract—This paper introduces analytical expressions for the modeling of path-loss and shadow fading in residential indoor-to-outdoor scenarios. The formulas have been calibrated using channel power measurements at the radio frequencies of common cellular systems and are thus suitable for channel modeling in femtocell networks. The expressions presented here can be used as a simple propagation model in system-level simulators, as well as for comparison with other models. Furthermore, its compact formulation simplifies its use for theoretical studies of two-tier networks, while its empirical nature strengthens its validity.

Index Terms—indoor, outdoor, empirical, propagation model, femtocell

I. INTRODUCTION

LOW power base stations, also known as femtocell access points (FAPs), have appeared in recent years as a feasible solution to the indoor coverage and capacity problem [1]. However, the co-channel deployment of a femtocell network tier over a macrocell network tier introduces challenges to the macrocellular network planning process. These include, among others, cross-tier interference. In view of this, most studies on interference mitigation in two-tier networks rely either on system-level simulations (SLS) [2] or on theoretical models [3] of the network topology. Further, these works require propagation models that shape the physical behavior of the cross-tier radio channel.

Numerical methods such as ray tracing and the finite-difference time-domain (FDTD) have shown acceptable performance and accuracy when used in SLS [4]. These are interesting since they facilitate the modeling of the scenario during simulation, thus avoiding the need for a channel model indoors and a different one outdoors. However, these techniques are intended to be run on computing platforms, thus lacking their formulations mathematical flexibility for their implicit use in analytical studies.

Hence and for the purpose of mathematical network characterization, analytical expressions based on empirical power measurements in these scenarios are necessary. Such models would facilitate not only analytical and simulation-based studies of femtocell networks, but also serve as a measurements-backed propagation model for comparison with others.

Manuscript received May 11, 2010; revised June 15, 2010; accepted July 05, 2010. This work was supported by the EU FP6 RANPLAN-HEC project on 3G/4G Radio Access Network Design under Grant MEST-CT-2005020958.

The authors are with the Centre for Wireless Network Design (CWIND), Institute for Research on Applicable Computing (IRAC), University of Bedfordshire, Luton LU1 3JU, U.K. (e-mail: alvarovalcarce@gmail.com).

Color versions of one or more of the figures in this letter are available online at <http://ieeexplore.ieee.org>.

Digital Object Identifier 10.1109/LAWP.2010.2058085

A. Related work

Most approaches to outdoor-to-indoor propagation separate indoor attenuation from that outdoors [5]. However, the indoor-to-outdoor literature is scarce. For instance in 2007, the WINNER project studied the indoor-to-outdoor channel [6] via measurements in a university campus. Initial empirical results on the behavior of indoor microcells were then revealed. Such measurements were performed in the 2 – 6 GHz range with indoor antenna heights at 2 – 2.5 m. Then, the data was used to adapt a COST231-project formula to the measured frequencies. However, lower frequencies such as 900 MHz (of interest in GSM femtocells) were left out of the model.

In [7], an analytical expression for the additional losses at the indoor/outdoor interface was developed to be used with separate propagation models for the prediction of the full path loss. However, this was based on statistics extracted from ray-tracing simulations and it has not been validated by measurements. According to its authors, it must hence be considered as a preliminary model.

B. Contribution

The current paper fills in some of the gaps left by the previously mentioned works:

- Unexplored frequency range for indoor-to-outdoor.
- Ground-floor transmitter in two measurement sites.
- Transmitter location outdoors, in outer and in inner room.
- No need for additional models in link evaluation.
- Model based on measurements instead of simulations.

By performing several measurement campaigns of channel power in two different residential areas, a measurements database has been constructed. Thus, the current model is suitable for application in scenarios similar to those described in this paper. The frequencies of interest for current and future cellular communication systems have been measured in setups that resemble the downlink propagation path in femtocells. Then, an empirical formula has been calibrated to reproduce the observed behavior in terms of path-loss and shadow fading.

The techniques for path loss fitting are well known. Nevertheless, the contributions of this work lie on the uninvestigated indoor-to-outdoor channel, as well as on the industry and research community need for femtocell propagation models.

II. MEASUREMENTS SETUP

A. Equipment

The transmitter, with an output power of $P_{tx} = 19 \text{ dBm}$, is a vector signal generator MG3700A from Anritsu. In order



Fig. 1. Receiver and transmitter with the SVD2-915/432 antennas.

to perform continuous wave (CW) measurements, it radiated a continuously oscillating signal at the surveyed frequencies: 900 MHz, 2 GHz, 2.5 GHz and 3.5 GHz.

Slim flexible dipoles of the SVD2 series from Cobham were used as antennas and connected directly to the RF output of the transmitter and the RF input of the receiver (see Figure 1). This eliminates uncertainties in the measurements due to cable losses at high frequencies. The antenna models for the different center frequencies were SVD2-915/432 ($f = 900$ MHz), SVD2-2000-NM/958 ($f = 2$ GHz), SVD2-2500/869 ($f = 2.5$ GHz) and SVD2-3450/426 ($f = 3.5$ GHz). All of these have similar radiation patterns at their operating frequencies, being nearly omniazimuthal, with a vertical beamwidth of 80° and a maximum gain of $G = 2$ dBi. The measurements device was a portable spectrum analyzer MS2721B from Anritsu.

B. Location

The measurement sites were two residential neighborhoods in a medium-size British town (see Figure 2). The houses have 2 - 3 floors with an average height of 6 m, and the main construction materials are brick for the outer walls and wood, chipboard and plaster for the indoors. All measurements were taken during sunny days in November 2009. The height of the transmitter antenna measured from the ground floor was 1 m throughout all measurements. It was first placed outdoors in front of the outer facade of a terraced house to measure the attenuation due to outdoor propagation. Then, it was moved into two different rooms of the ground floor. The first room was immediately adjacent to the house's outer facade, while the second one was an inner room, two walls apart from the street. This allows for a separate analysis of the attenuation due to outdoor propagation and that corresponding to the indoors.

FAPs leak power outdoors through the premises front facade, thus causing interference to macrocells in the adjacent street-canyon of the residential area. Hence, the measurements have been performed in the street immediately adjacent to the premises and until distances from the outer wall at which the received channel power drops below -110 dBm (10 dB security margin from the noise floor at -120 dBm). This is approximately 110 m at 2 GHz when the transmitter is in the inner room, which is akin to a residential 3G femtocell coverage radius when four users are served [8].

C. Measurements procedure

Prior to each measurement, an spectral scan was performed in the bands of interest to avoid interference from third-party

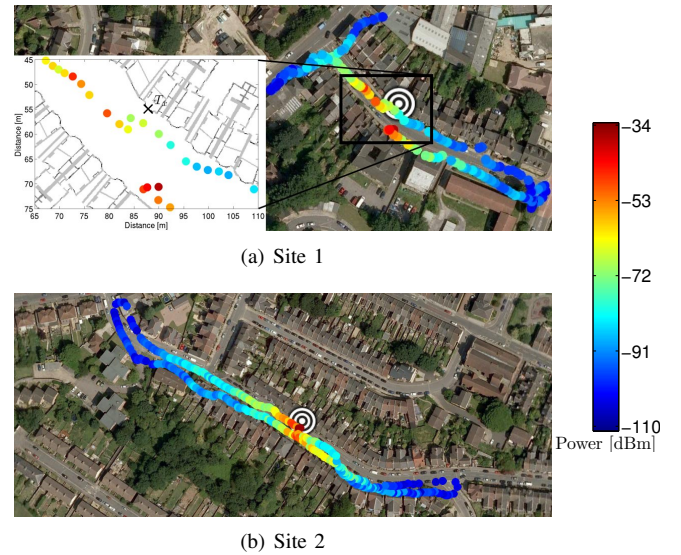


Fig. 2. Aerial view of the measurement sites and the measured power when the transmitter is in the outer room. $P_{tx} = 19$ dBm and $f = 2$ GHz. The indoor/outdoor interface point is indicated with a cross in Site 1.

sources. Then the measurements consisted, for each location, on the frequency sweep of a 1 kHz band centered at the previously described frequencies. This avoids errors due to frequency instability at the transmitter, as well as to Doppler shifts. The receiver was set up to record one spectral value every 9 Hz. Then, the received power P_{rx} was computed by integrating the recorded points over the spectral band. The measurements device was carried by hand in order to resemble realistic usage of user equipment (UE). The user walked slowly and uninterruptedly along the street to suppress small-scale fading and the receiving antenna height was 1.20 m.

The measurements locations were resolved with a GPS receiver (see Figure 2). On average, 283 locations were visited when the transmitter was in the inner room, and 386 locations when in the outer one. Since four frequencies and three transmitter locations were surveyed, this adds up to nearly 4000 data values across all locations. However, after the removal of points with GPS errors and noise-bins (received power less than 10 dB above the noise floor), a total of 3897 points were finally used for model calibration.

III. CALIBRATION OF EMPIRICAL MODEL

As with most empirical propagation models, the formulation of path-loss and shadow fading has been separated. Then, the power attenuation A in dB at a given location is

$$A = PL + R \quad (1)$$

where PL is the mean path loss and R is the shadow fading factor in dB. For the calibration of the empirical formula, the data from both measurement sites has been used. Then, in section III-C, the prediction error is calculated independently in both sites to assess the validity of the model across different measurement localities. The measurements-based calibration of these parameters is explained in the following.

TABLE I
PATH LOSS FITTED PARAMETERS

PL_0	d_0	a	b	c	p_1	p_2	α	β
62.3	5	$3.3 \cdot 10^{-4}$	6.0	3.2	-1.8	10.6	5.8	-5.5

A. Path loss

Since the same type of antennas were used in both transmitter and receiver, the p^{th} empirical path loss value in dB is determined from the power measurements as

$$PL_p = P_{tx} + 2G - P_{rx,p} \quad (2)$$

where $P_{rx,p}$ is the p^{th} received power value in dBm.

In indoor-to-outdoor scenarios, PL can be separated in two parts: First, the attenuation PL_i from the transmitter until the indoor/outdoor interface at the house's outer wall. Secondly, the outdoor attenuation PL_o from the facade til the receiver in the street. Then, the path loss is

$$PL = PL_i + PL_o. \quad (3)$$

To separate the indoor attenuation from the outdoor one, PL_o is first calibrated with the data collected when the transmitter is outside of the house at the interface point. This is done using the exponential model

$$PL_o = PL_0 + 10\gamma \log_{10} \left(\frac{d}{d_0} \right) \quad (4)$$

with PL_0 being the intercept value of the path loss model at a distance $d_0 = 5$ m from the transmitter. This yields $PL_0 \approx 62.3$ dB and a frequency-dependent attenuation exponent γ to be determined. The best fit of γ was found to follow a power relationship with frequency:

$$\gamma(f) = a \cdot f^b + c \quad (5)$$

where f is given in GHz and the shape parameters a , b and c are given in Table I. This fit is further illustrated in Figure 3.

Then, the transmitter is moved into the house and the overall attenuation is measured. The attenuation rise over the previous case is due to indoor propagation, which is subject to rich multipath reflections and complex modeling. However, the objective here is to model the effect of the transmitter's indoor location with respect to the outer facade and its impact onto the overall power attenuation. Hence, the expression for the indoor loss PL_i is based on a simplified formulation that depends on the number N_w of walls between the transmitter and the street.

This way, the attenuation PL_i due to indoor propagation is shown on Figure 3 for two cases: transmitter in outer room ($N_w = 1$) and transmitter in the next-to outer room ($N_w = 2$). In this case, the best fit to PL_i depends quadratically on the frequency and linearly on the number N_w of walls:

$$PL_i = \begin{cases} 0, & \text{if } N_w = 0 \\ p_1 f^2 + p_2 f + p_3(N_w), & \text{if } N_w \in [1, 2] \end{cases} \quad (6)$$

$$p_3(N_w) = \alpha \cdot N_w + \beta. \quad (7)$$

Note that $N_w \in [0, 2]$. Cases in which the transmitter is located deeper into the house have not been measured and are thus not observed by this model. The obtained model parameters

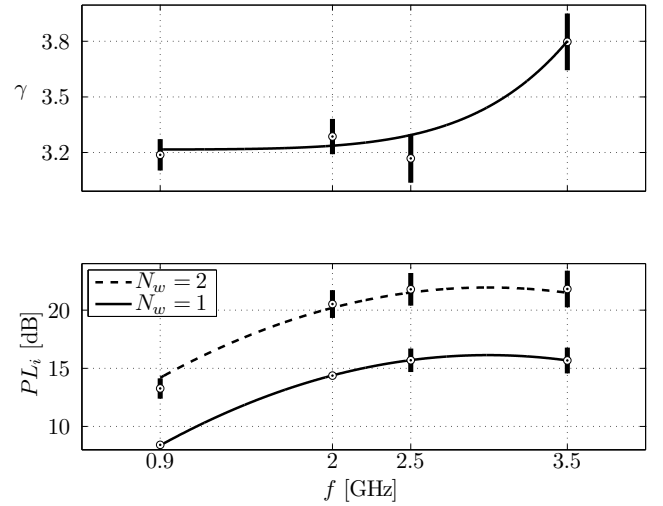


Fig. 3. Model and measured parameters with 95% confidence intervals.

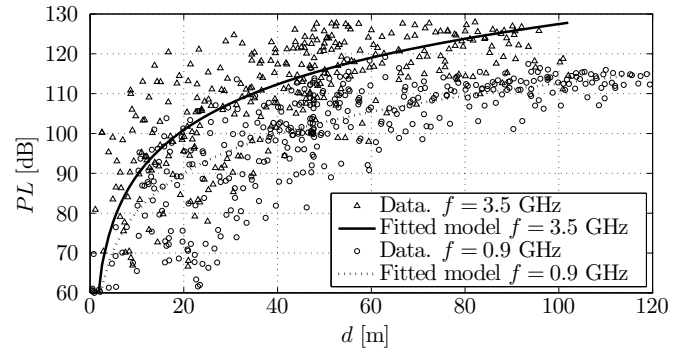


Fig. 4. Measurements and model with transmitter in outer room ($N_w = 1$).

are those in Table I and the fitted indoor path loss PL_i is illustrated on Figure 3 along with the measurements.

All of the parameters described by the previous equations have been fitted to the data via a *Trust Region* optimization algorithm. The residual of a data value with index p is defined as the difference between the empirical value PL_p and that predicted by the fitted parametric curve \widehat{PL}_p . Then, the objective function to be minimized was the sum S of the absolute value of the residuals¹

$$S = \sum_{p=1}^{N_p} |PL_p - \widehat{PL}_p| \quad (8)$$

where N_p is the number of measurement points. Compared to a Least Squares fit, this method reduces the effect of large outliers on the final fit. Some of the obtained curves are then shown on Figure 4 along with part of the measured data.

B. Shadow fading

Shadow fading is modelled as the random variation of the received power around the mean and is thus based on the residuals of the previous path loss fit. These variations include all large-scale uncontrolled phenomena within the propagation

¹This regression method is known as the least absolute residuals (LAR).

TABLE II
RMSE IN DB OF THE PATH LOSS MODEL

	f [GHz]	0.9	2	2.5	3.5
Site 1	$N_w = 0$	8.7	10.7	9.8	9.0
	$N_w = 1$	8.4	9.5	9.4	7.1
	$N_w = 2$	6.3	9.7	9.1	11.7
Site 2	$N_w = 0$	9.6	9.7	9.8	11.1
	$N_w = 1$	9.2	11.5	10.4	11.9
	$N_w = 2$	11.4	11.1	11.5	12.4

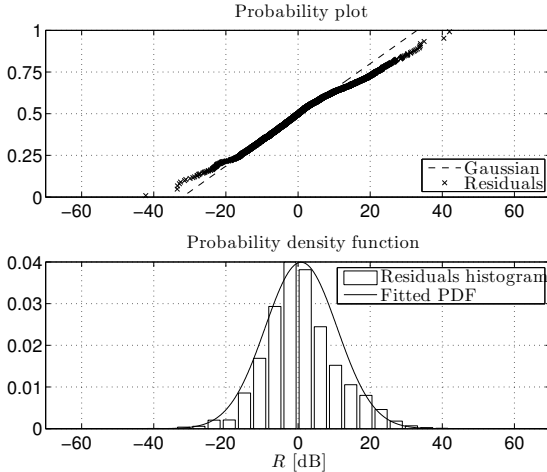


Fig. 5. Fitted and scaled empirical shadow fading distribution.

channel such as moving obstacles and scatterers. The objective is thus to describe statistically the distribution of the residuals, which are equivalent to the shadow fading factor R in dB.

It has been found that a Gaussian distribution $\mathcal{N}(\mu, \sigma^2)$, with μ the mean and σ the standard deviation, approximates well the behavior of R . This is reasonable since the errors of the path loss fit from the Trust Region algorithm are nearly Gaussian distributed. The parameters of the normal distribution are then obtained from the residuals using maximum likelihood estimation (MLE). It must be remarked that, for the residuals of the previous path loss fit, no major variation of μ and σ has been observed at the different tested frequencies and indoor scenario settings ($N_w \in [0, 2]$). This way, the obtained parameters for the normal distribution of R are

$$\begin{aligned} \mu_R &\approx 0.85578 \text{ dB} \\ \sigma_R &\approx 9.99414 \text{ dB} \end{aligned} \quad (9)$$

with standard errors (confidence intervals)

$$\begin{aligned} \sigma_{\mu_R} &\approx 0.160096 \text{ dB} \\ \sigma_{\sigma_R} &= 0.113227 \text{ dB}. \end{aligned} \quad (10)$$

This is illustrated in Figure 5, which shows the obtained probability density function (PDF) and the residuals histogram.

C. Model validation

The accuracy of the path loss fit is evaluated using the root mean squared error (RMSE), which considers both measurements and model predictions (see Table II). Note that the data

is subject to shadow fading. Hence, the RMSE can also be seen as the standard deviation of the measurements around the model's prediction due to shadow fading.

For comparison, the RMSE of the deterministic model in [4] was 6 dB at $f = 3.5$ GHz, while [6] claimed a standard deviation of 7 dB at 2 – 6 GHz. These are, however, for the case $N_w = 1$ and with further topological differences. The current model has an RMSE of 10 dB, thus bringing in a new result on the behavior of shadow fading in these scenarios.

IV. CONCLUSIONS

This letter has presented a path loss and shadow fading model to be used in analytical studies of two-tier wireless networks. The proposed formulas have been calibrated using power measurements in two residential scenarios, thus increasing its reliability for such settings. One useful feature of this model is that the surveyed spectral range comprises some of the most commonly used radio frequencies in cellular wireless systems. This allows for its direct application to the study of the already existing 3G as well as future 4G femtocells.

For example, with this model it is straightforward to estimate the cross-tier interference level from a closed subscriber group (CSG) 3G femtocell ($f = 2$ GHz) with $P_{tx} = 15$ dBm on a non-subscriber located $d = 10$ m from the premises. If the FAP is in the outer room, then $N_w = 1$ and $P_{rx} \approx -71$ dBm. Using then the shadow fading distribution above, it can also be calculated that $R \in (-25, 27)$ dB for 99% of the time. This helps in the estimation of extreme interference levels at given distances from the femtocell premises.

Furthermore, the implementation of this model in system-level simulators is quick and simple, thus avoiding the need for complex propagation models. Ray-tracing and finite-difference models usually achieve higher precisions in these scenarios. However, measurements are not always available for their calibration. Hence, the model introduced here also serves as a reliable alternative and is useful for comparison purposes of geometrical as well as other types of propagation models.

REFERENCES

- [1] J. Zhang, G. De La Roche, A. Valcarce, D. López-Pérez, E. Liu, and H. Song, *Femtocells: Technologies and Deployment*. Wiley, Jan. 2010.
- [2] D. Lopez-Perez, A. Valcarce, G. De La Roche, and J. Zhang, "OFDMA Femtocells: A Roadmap on Interference Avoidance," *IEEE Communications Magazine*, vol. 47, no. 9, pp. 41–48, Sep. 2009.
- [3] V. Chandrasekhar and J. G. Andrews, "Uplink Capacity and Interference Avoidance for Two-Tier Femtocell Networks," *IEEE Transactions on Wireless Communications*, February 2008.
- [4] A. Valcarce *et al.*, "Applying FDTD to the coverage prediction of WiMAX femtocells," *EURASIP Journal on Wireless Communications and Networking*, Mar. 2009. [Online]. Available: <http://www.hindawi.com/journals/wcn/2009/308606.html>
- [5] M. Döhler, "An Outdoor-Indoor Interface Model for Radio Wave Propagation for 2.4, 5.2 and 60 GHz," Master's thesis, Kings College London, 1999.
- [6] P. Kyösti *et al.*, "WINNER II Channel Models," WINER II Public Deliverable, Sep. 2007.
- [7] "Predicting coverage and interference involving the indoor-outdoor interface," Ofcom, Project SES-2005-08, Tech. Rep., Jan. 2007.
- [8] H. Claussen, L. T. W. Ho, and L. G. Samuel, "An overview of the femtocell concept," *Bell Labs Technical Journal*, vol. 13, no. 1, pp. 221–245, May 2008.